Carbonyl-precursor-based W/Al_2O_3 and CoW/Al_2O_3 catalysts: characterization by temperature-programmed methods

Mika Suvanto, Jarkko Räty and Tapani A. Pakkanen *

Department of Chemistry, University of Joensuu, PO Box 111, FIN-80101 Joensuu, Finland

Received 29 March 1999; accepted 5 August 1999

Carbonyl-precursor-based W/Al_2O_3 and bimetallic CoW/Al_2O_3 catalysts were prepared by gas-phase adsorption in a fluidized-bed reactor. The surface species formed during the gradual and controlled preparation process were studied by temperature-programmed methods. Interactions on the surface were investigated as a function of metal loading by temperature-programmed oxidation (TPO) and oxygen pulse chemisorption (PCO). A clear relationship was observed between decarbonylation treatment and the tungsten species formed. Total acidity of the samples was determined by temperature-programmed desorption of ammonia (NH_3-TPD). The NH_3-TPD measurements, together with previous activity studies, suggest a relationship between total acidity and hydrotreating activity. The results of PCO and NH_3-TPD measurements indicate that when the controlled gas-phase preparation method is applied to zerovalent carbonyl precursor, the unfavourable formation of tungsten oxide can be minimized.

Keywords: tungsten hexacarbonyl, dicobalt octacarbonyl, alumina, gas-phase preparation, TPO, PCO, NH_3-TPD

1. Introduction

Tungsten hexacarbonyl adsorbed on alumina has been studied as a catalyst in metathesis [1,2], Fischer–Tropsch synthesis [3] and alkene hydrogenation [4]. Whilst tungsten-oxide-based catalyst has been widely studied in the hydrotreating process [5–18], use of the carbonyl-precursor-based catalyst in the reaction is rare. We have nevertheless achieved promising activities with tungsten-hexacarbonyl-based hydrotreating catalyst, especially, when a small amount of cobalt was added as promoter [19]. Traditional tungsten catalyst is commonly prepared by a liquid-phase method such as impregnation with hexavalent salt of tungsten. The formed tungsten oxide species are difficult to reduce [17,18,20–27] and difficult to activate by sulfurization [7,17,18,28–30] at moderate temperature. A more promising route may thus be the use of zerovalent precursors, such as tungsten and cobalt carbonyls, in a gradual and controlled gas-phase deposition where oxidation during preparation can be avoided.

Production of a good catalyst demands careful control of the preparation and careful monitoring of surface processes. Several studies on the surface chemistry of alumina-adsorbed $W(CO)_6$ have been reported elsewhere [31–40]. The main purpose of these earlier measurements was to clarify the formation of subcarbonyl species during decarbonylation. Neither the control of the preparation process nor the achieved metal loading was very good, however. The surface properties of the decarbonylated system have seldom been discussed.

Temperature-programmed methods are commonly used in studying the reactivity and properties of alumina-adsorbed tungsten oxide catalysts, but they have not been extensively applied for carbonyl-precursor-based systems except where the decarbonylation process was followed by temperature-programmed desorption (TPD) measurements [33–36]. In earlier work we studied the reduction behaviour of tungsten-hexacarbonyl-based catalyst by temperature-programmed reduction (TPR) [19]. The aim of the present work was to study the surface properties of carbonyl-precursor-based W/Al_2O_3 and CoW/Al_2O_3 catalysts through temperature-programmed oxidation treatments (TPO, PCO) and by temperature-programmed desorption of ammonia (NH_3-TPD) in the case where all carbonyl ligands were removed.

2. Experimental

2.1. Reactants and preparation method

$W(CO)_6$ supplied by Aldrich and $Co_2(CO)_8$ supplied by Fluka were used as reactants without further purification. The aluminium oxide (75–60 mesh, 195 m^2/g) supplied and reported by Akzo provided the support. For the partial dehydroxylation, the support was preheated at 500 °C in vacuum for 10 h. After pretreatment, all handling of support material was made in a nitrogen glove box ($O_2 \approx 0.5$ ppm and $H_2O \approx 0.1$ ppm).

The alumina-supported tungsten and bimetallic tungsten cobalt samples were prepared in a fluidized-bed reactor by gas-phase adsorption. Tungsten hexacarbonyl was vaporized at 90 °C and transferred to the fluidized-bed reactor under nitrogen flow (99.999%, AGA). The temperature of the fluidized-bed reactor and alumina support was 100 °C during deposition. A pulse technique was used to adjust the

---

* To whom correspondence should be addressed.

tungsten loading to targeted level. A partial decarbonylation between the deposition pulses was applied to reduce the formation of steric hindrance and to avoid oxidation during preparation. A single $W(CO)_6$ deposition pulse took 2 h and the CO ligands were partially removed after each carbonyl precursor pulse by heating the samples at 200 °C for 10 h. After the final $W(CO)_6$ pulse, all carbonyl ligands were removed by applying hydrogen (99.999%, AGA) at 450 °C for 5 h. A more detailed description of the reactor system and the gradual methods employed can be found elsewhere [41].

Pure Co/Al_2O_3 samples and CoW/Al_2O_3 catalysts were prepared by depositing dicobalt octacarbonyl under CO flow (99.997%, Messer). For bimetallic CoW catalysts, all tungsten steps were made before the deposition of cobalt carbonyl. The sublimation temperature for $Co_2(CO)_8$ was 45 °C and the duration of a single cobalt carbonyl pulse was 5 h. Carbonyl ligands were removed under hydrogen flow at 200 °C for 5 h.

The tungsten loading of alumina-supported samples ranged from 1.1 to 5.5 wt%. (The metal contents of samples are indicated below as W-1.1, etc.) In the case of pure Co/Al_2O_3 sample and bimetallic CoW/Al_2O_3, one deposition decarbonylation pulse was used to produce low-to-moderate 0.3 wt% cobalt loading.

2.2. Characterization of the samples

Tungsten loading of samples was determined with an energy dispersive X-ray fluorescence spectrometer (ACAX 300 EDXRF). Cd(109) radioisotope was used as the source of radiation. Measurement time was 100 s and the resolution of measurements was 0.15 keV.

The crystallinity of tungsten samples was determined with powder X-ray diffraction. Diffraction data were collected on a Bruker AXS D8 Advance diffractometer equipped with Göbel mirrors and Soller slits using Cu Kα radiation ($\lambda = 1.542$ Å).

Temperature-programmed oxidation, oxygen pulse chemisorption and ammonia desorption measurements were carried out with a Micromeritics AutoChem 2910 analyser equipped with a TCD detector. The measurements are based on study of the difference in thermal conductivity between a reference gas flow and a flow running through the sample.

During temperature-programmed oxidation measurements, a 10 °C/min temperature ramp was applied and the final temperature was 500 °C. The flow rate of oxidative 5% O_2/He (99.9999%, AGA) mixed gas was 40 ml/min.

In the case of oxygen pulse chemisorption, two different oxidation temperatures, 250 and 500 °C, were applied. Ar (99.9999%, AGA) was used as a carrier gas (10 ml/min). Dosing of oxygen (99.9999%, AGA) was carried out with a 1 ml gas loop and the oxygen flow rate through the loop was 10 ml/min. Before the measurements, the volume of the injection loop was calibrated by reference volume injection.

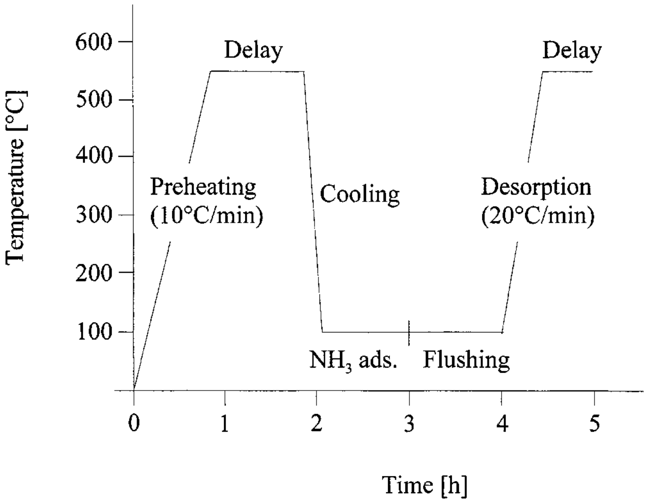

Figure 1. Temperature program for NH_3-TPD studies.

He (99.9999%, AGA) was used as a carrier gas in ammonia temperature-programmed desorption studies. 10% NH_3/He mixed gas (AGA) was used as adsorbate. The flow rate of the carrier and mixed gases was 30 ml/min. The system was calibrated by monitoring the signals caused by addition of known amounts of NH_3 to carrier gas. During desorption, a 20 °C/min temperature ramp was applied and the final temperature was 550 °C. A more detailed description of the applied desorption program is given in figure 1.

IR [42–45], microcalorimetric [46–48] and recently also TPD [15,49,50] studies of ammonia are widely used techniques for probing the acidic properties of alumina and alumina-supported catalysts. Because of its small size and strong basicity, ammonia is suitable for the detection of almost all the acidic sites on a porous material. The main disadvantage of using ammonia as a probe molecule is that it can interact with the surface in several ways, so that the response of different sites cannot easily be distinguished. However, even though the resolving of the distribution and number of different alumina acidic sites by ammonia adsorption studies is a complex task, the approach provides an effective tool for comparing the overall acidity of different supports and catalysts.

3. Results and discussion

3.1. Temperature-programmed oxidation

The TPO profiles of two W/Al_2O_3 samples with different tungsten loadings are presented in figure 2. For comparison, the oxidation pattern of alumina-supported cobalt is also included. The interpretation of TPO patterns is solely qualitative and total O_2 uptake was not quantified. However, the effect of tungsten loading on the oxidation is evident. The O_2 consumption in an oxidative process increases the thermal conductivity of gas flow (5% O_2/He) which can be seen as a positive deviation of trace. Accordingly, at low tungsten loading (W-1.1) only a slight O_2 consumption

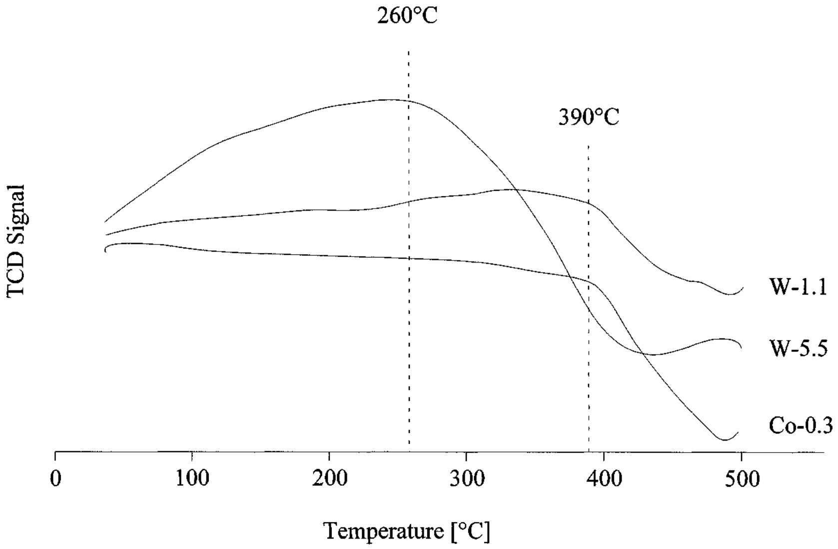

Figure 2. TPO profiles of alumina-adsorbed tungsten and cobalt samples.

was observed. When the tungsten loading was increased to 5.5 wt% (W-5.5) the O_2 uptake was more stronger. This difference in O_2 uptake can be attributed to the increased metal loading.

The oxidation results reported in the literature show that the oxidation of alumina-supported cobalt-nitrate-based catalysts may proceed via CoO and Co_3O_4 under 600 °C [42]. However, in our case the TPO pattern of the cobalt sample with low metal loading did not show any upward deviation due to O_2 consumption. This suggests that for carbonyl-precursor-based Co/Al_2O_3 the oxidation steps occurred immediately when the oxidative gas mixture was passed through the sample, during the initial stabilization period (the period during which the slope of the base line stabilized) before the detection was initiated. It should be added that the low cobalt loading (0.3 wt%) applied in our case may also affect the situation.

The oxidation that occurred during decarbonylation (as a consequence of a redox reaction between carbonyl complex and surface hydroxyls) may also be relevant. Oxidation would likewise lead to a situation where the oxidation was not detected. In any event, in an attempt to minimize the effect of oxidation during the preparation, the carbonyl ligands were eliminated from adsorbed tungsten and cobalt complexes at high temperature under reducing atmosphere (hydrogen flow).

The negative deviations of profiles can be seen around 260 °C for W-5.5 and at 390 °C for W-1.1 and Co-0.3. This indicates liberation of gaseous compounds which have lower thermal conductivities than helium (the main component of the gas mixture). The source of these gases can be attributed to decomposition of adsorbed carbonate and formiate species formed during decarbonylation.

3.2. Oxygen pulse chemisorption

Pulse chemisorption results for the CoW catalyst at 250 and 500 °C are set out in table 1. As can be seen, O_2 consumption was clearly higher at 250 °C (1.92 ml/g sample) than at 500 °C (1.36 ml/g sample). Evidently, at higher temperature the oxygen adsorption is partly prevented by the excess energy of the system. It may also be that, at higher temperature, the stability of the adsorbed oxygen begins to decrease, which further increases the amount of desorbed O_2 molecules.

Table 1
O_2 pulse chemisorption results of bimetallic CoW catalyst at 250 and 500 °C.

Sample	Metal content (wt%)		Oxidation temperature	O_2 uptake
	W	Co	(°C)	(ml/g sample)
CoW/Al_2O_3	5.5	0.3	250	1.92
CoW/Al_2O_3	5.5	0.3	500	1.36

Oxygen pulse chemisorption (PCO) provides an effective way to study the effect of decarbonylation conditions on surface species. Table 2 summarizes the results of PCO measurements where carbonyl ligands of $W(CO)_3/Al_2O_3$ samples were removed under argon or hydrogen atmospheres. For comparison, the table includes the oxidation result in the case where the PCO study was made without removing all of the carbonyls. The tungsten loading of each sample was the same (4.7 wt%) and the oxidation treatment was carried out at 250 °C.

Inspection of the results reveals that the amount of consumed O_2 was clearly lower for the sample treated under Ar at 500 °C than for the sample where oxidation was carried out directly, without heating. Even though it is known that hexacarbonyl compound adsorbed on the surface may form $W(CO)_2O_2$ and $W(CO)_2(O_2)_2$ complexes when reacting with oxygen [53], the observed four-fold difference in O_2 uptake was too great to be due only to these oxygen complexes. The calculated dispersions of these samples also differ noticeably. Even though the exact stoichiometry for oxygen adsorption is not known (it is assumed to be 1 : 1) the given dispersion values

Table 2
Effect of decarbonylation conditions on the oxidation of W species formed on alumina.

Sample W (4.7 wt%)	Complete decarbonylation treatment (gas/temperature)	O_2 consumption (ml/g sample)	O_2/metal molar ratio	Dispersion[a] (%)
$W(CO)_3/Al_2O_3$	Ar/500 °C	0.26	0.04	4
$W(CO)_3/Al_2O_3$	–	1.16	0.20	20
$W(CO)_3/Al_2O_3$	H_2/450 °C	1.38	0.24	24

[a] Dispersions were derived from O_2/metal molar ratios [52].

Table 3
O_2 pulse chemisorption results for alumina-supported W, Co and CoW samples at 250 °C.

Sample	O_2 consumption (ml/g sample)	Content $\times 10^{-2}$ (mmol)		O_2/metal molar ratio
		O_2	Metal	
Co-0.3	0.35	1.5	5.1	0.30
W-1.1	0.10	0.4	6.0	0.07
W-3.4	0.63	2.8	18.5	0.15
W-5.5	1.43	6.4	29.9	0.21
CoW-0.3/5.5	1.92	8.6	35.0	0.24

can be compared since the samples were of similar origin.

The dispersion results suggest in accordance with the literature [34] that the three carbonyl ligands left on the metal centre are able to keep most of the bonded tungsten atoms molecularly dispersed. When these remaining carbonyls are removed by heating under Ar, agglomeration begins and the O_2 consumption decreases.

Comparison of all three measurements reported in table 2 nevertheless suggests that the difference in O_2 uptake more probably is due to oxidation during decarbonylation treatment than to the difference in dispersion. The first sample was treated under inert Ar gas at moderate-to-high temperature, which may lead to redox reaction, and, therefore, the sample was oxidized before pulse chemisorption treatment. In this reaction surface hydroxyls could be the source of oxygen. This is in agreement with our previous IR studies where we showed that complete decarbonylation under inert N_2 flow may lead to the formation of tungsten oxide species on alumina surface [54].

When carbonyl ligands were not removed the O_2 uptake increased noticeably but partly as a consequence of the formation of oxidized carbonyl complexes. The bottom row in table 2 shows the effect of hydrogen treatment. The over five-fold difference in O_2 consumption between samples treated under argon and hydrogen is too great to be due to the 50 °C temperature difference. Evidently, when decarbonylation is made under reducing atmosphere instead of argon, the oxidative surface reaction is prevented or at least minimized.

The oxygen pulse chemisorption results for alumina-supported W, Co and CoW samples at 250 °C are shown in table 3. All samples discussed here were decarbonylated completely under hydrogen flow before PCO measurements. As expected, in the pure tungsten samples O_2 uptake increased with the tungsten loading. In the case of the cobalt sample with low metal loading the O_2 consumption was relatively high due to its better oxidation capability. The bimetallic CoW catalyst showed the highest O_2 uptake (1.92 ml/g sample) within the studied series. Note that this value is higher than the sum of the values for the monometallic (Co-0.3 and W-5.5) samples. This indicates that the surface structure of the bimetallic system differs from the mixture of pure components and points to the formation of bimetallic phase.

The last column in table 3 shows the calculated O_2/metal ratios. Comparison of the series of pure tungsten samples reveals that the proportion of tungsten particles that are reactive towards oxygen treatment increases with metal loading. Evidently, larger tungsten particles begin to form at higher surface concentration, and this leads to the situation where part of the interactions with the surface are replaced by interactions between adjacent tungsten atoms. The diminishing of the strong surface effect on the outermost parts of larger tungsten species can then be seen as higher reactivity towards oxygen treatment. Even though the dispersion begins to decrease as a function of tungsten loading, X-ray diffraction measurements did not indicate formation of crystalline tungsten particles on the surface.

All these oxidation studies are in good accord with our previous TPR (temperature-programmed reduction) and hydrotreating activity studies [19]; the increase of tungsten loading changes the surface dispersion and this affects the surface reactivity towards different kinds of treatment and reactants. In our previous studies we noticed that the amount of consumed H_2 or H_2S or the relative activity per adsorbed tungsten decreased as the metal loading increased [19]. However, the results of oxygen treatment experiments revealed that the O_2/metal molar ratio increased as a function of tungsten loading. The difference suggests that the surface chemistry is different for reduction (H_2 uptake) and oxidation (O_2 uptake) processes. The amount of adsorbed hydrogen or number of active sites is more directly controlled by dispersion and the outermost surface layer. The oxygen uptake was greater when at least part of the interactions of metal species with the surface were diminished. At low metal loadings, well dispersed tungsten particles were surrounded by many surface hydroxyls and oxo groups, making the particles less reactive towards oxygen.

3.3. Temperature-programmed desorption of ammonia

We performed ammonia desorption experiments to determine the total acidity of samples and to study whether there is a correlation between acidity of the carbonyl-based tungsten catalysts and the hydrotreating activity that we observed in our previous work [19].

The NH_3-TPD profiles of pure alumina support and of tungsten catalysts with increasing metal loading are presented in figure 3. The shape of the pure support profile is in good agreement with the results of alumina NH_3-TPD studies reported in the literature [15,49,50] even though the positions of maxima were slightly shifted to higher temperatures due to the higher heating rate (20 °C/min in our case). The dominating structure of all profiles is one broad and strong band at about 220 °C, which can be assumed to be due to NH_3 desorption from a relatively weak acidic site. Besides this dominating peak, alumina shows a shoulder slightly below 400 °C and a fairly broad but weak band when the temperature was held at 550 °C. These two desorption peaks may be assigned to medium and strong acid sites, respectively.

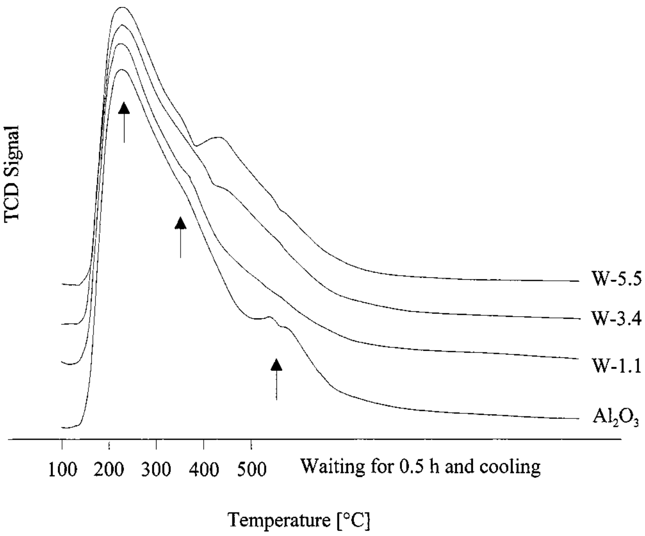

Figure 3. NH_3-TPD profiles of pure alumina support and tungsten catalysts with different metal loading.

When tungsten was deposited (W-1.1), the portion of the most acidic alumina centres decreased. This can be seen as a diminishing of the peak in the highest temperature region. The TPD profiles of W-3.4 and W-5.5 revealed a similar trend, in good agreement with the reported NH_3-TPD profiles for alumina-deposited tungsten oxo species [15].

When tungsten loading was increased up to 3 wt% (W-3.4 and W-5.5), a new desorption maximum appeared at about 430 °C. This new peak in the region of medium acidic sites indicates that the portion of these sites increases at higher tungsten loadings.

To obtain more information about the acidic properties of the different systems, we estimated the total acidity from the area of measured TPD patterns. As figure 4 shows, the amount of desorbed NH_3 was lowest at low tungsten loading and the total acidity of W-1.1 was clearly lower than that of the pure support. This is in good agreement with the corresponding TPD pattern, which showed the amount of the most acidic sites to decrease with the deposition of tungsten.

When tungsten loading was increased the formation of new acidic sites led to increase in total acidity. However, the results presented in figure 4 reveal that even though the acidity of tungsten-based systems increased with metal loading, the acidity of the sample with the highest W content was still less than that of the pure alumina.

The addition of WO_3 to alumina has been reported to increase the total acidity of oxide-based systems even at low tungsten level [48]. Our finding that the total acidity decreased at the beginning of metal deposition indicates that the surface chemistry of the system differs from that of the

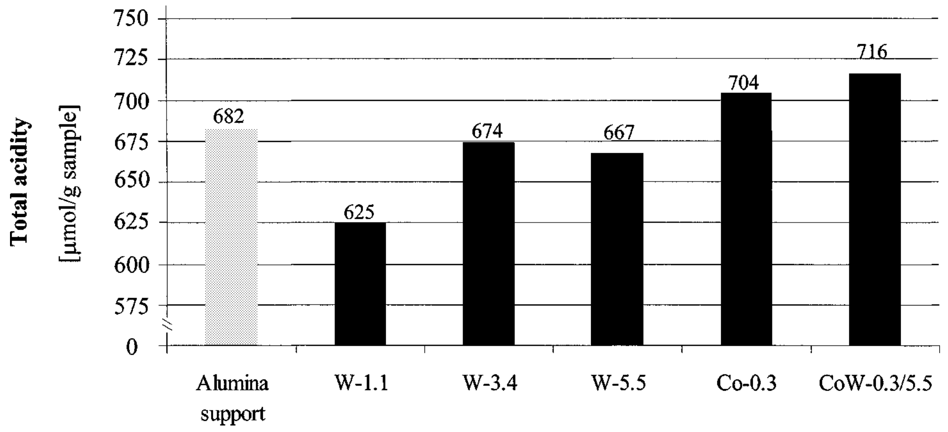

Figure 4. Total acidity of W, Co and CoW samples estimated from the area of measured NH_3-TPD patterns.

oxide-based systems. It is also suggested that the unwelcome formation of tungsten oxide surface species could be reduced through use of zerovalent carbonyl precursor and gas-phase preparation.

The amount of released NH_3 in the case of the pure cobalt sample shows that even low-to-moderate cobalt loading is sufficient to increase the total acidity of the Co/Al_2O_3 system. The addition of a similar amount of cobalt to the surface of W/Al_2O_3 catalyst (W-5.5) revealed a similar effect. Furthermore, judging from the column heights, the increase in acidity due to the addition of promoter was more pronounced for W-5.5 (from 667 to 716 μmol/g sample) than for the pure alumina support (from 682 to 704 μmol/g sample). This suggests that the tungsten particles which already are there on the alumina support affect the adsorption of cobalt.

In our recent study we reported hydrotreating activities achieved with carbonyl-precursor-based W/Al_2O_3 and CoW/Al_2O_3 catalysts [19]. Comparison of these activities with the amount of desorbed NH_3 suggests a relationship between these two surface processes. The bimetallic CoW catalyst that showed the best activity also had, according to NH_3-TPD, the highest acidity. The pure tungsten catalysts revealed a similar trend: the total activity and acidity were increased at higher substrate concentration. These findings are in good accord with activity and acidity results reported in the literature for oxide-based tungsten catalysts [5,18]. Benítez et al. [18] have shown that an increase in surface acidity of W/Al_2O_3 due to fluoride addition leads to increasing hydrotreating activity, especially for hydrodenitrogenation.

4. Conclusions

Temperature-programmed oxidation studies on carbonyl-precursor-based tungsten catalysts showed that the commencement of the oxidation varies with the metal loading.

Oxygen pulse chemisorption measurements were found to be a suitable tool for studying the effect of decarbonylation conditions on the surface species formed. The PCO results revealed that the use of reducing hydrogen atmosphere instead of argon during complete removal of carbonyl ligands from $W(CO)_3$ hinders the oxidation of adsorbed tungsten particles. The effect of the three remaining carbonyls on the molecular dispersion may also be relevant in this context.

The pulse chemisorption results show similar trends to the TPO profiles; the proportion of tungsten particles which are reactive towards oxygen treatment increases as a function of metal loading. This suggests that the strong effect of the surface diminishes at higher metal concentrations and that part of the interaction with the surface is replaced by interaction between adjacent tungsten particles.

NH_3-TPD profiles suggest that the portion of the most acidic surface sites decreases when tungsten is deposited. Increase in the tungsten loading up to 3 wt% led to the formation of a new desorption maximum at 430 °C, evidently due to the existence of new medium acid strength centres on the surface.

The evaluation of acidity through the NH_3-TPD measurements showed that low tungsten loading decreases the total acidity of the pure alumina support. The decrease in acidity, rather than the increase reported for oxide-based tungsten catalyst, suggests a difference in the surface species that are formed. As the tungsten loading was increased, so was the total acidity increased.

Comparison of the NH_3-TPD results for the pure tungsten and cobalt samples with those for CoW suggests the existence of a synergism in the case of the bimetallic system.

References

[1] J.L. Bilhou, A. Theolier, A.K. Smith and J.M. Basset, J. Mol. Catal. 3 (1977/78) 245.
[2] B. Gita and G. Sundararajan, J. Mol. Catal. A 115 (1997) 79.
[3] A. Cichowlas, E.P. Yesodharan and A. Brenner, Appl. Catal. 11 (1984) 353.
[4] D.A. Hucul and A. Brenner, J. Chem. Soc. Chem. Commun. (1982) 830.
[5] A. Benítez, J. Ramírez, J.L.G. Fierro and A. López Agudo, Appl. Catal. A 144 (1996) 343.
[6] P. Atanasova, T. Tabakova, Ch. Vladov, T. Halachev and A. López Agudo, Appl. Catal. A 161 (1997) 105.
[7] M. Breysse, M. Cattenot, T. Decamp, R. Frety, C. Gachet, M. Lacroix, C. Leclercq, L. de Mourgues, J.L. Portefaix, M. Vrinat, M. Houari, J. Grimblot, S. Kasztelan, J.P. Bonnelle, S. Housni, J. Bachelier and J.C. Duchet, Catal. Today 4 (1988) 39.
[8] F.J. Gil Llambías, J. Salvatierra, L. Bouyssieres and M. Escudey, Appl. Catal. 59 (1990) 185.
[9] M. Esen Kural, N.W. Cant and D.L. Trimm, J. Chem. Technol. Biotechnol. 47 (1990) 143.
[10] E. Kural, N.W. Cant, D.L. Trimm and C. Mauchausse, J. Chem. Technol. Biotechnol. 50 (1991) 493.
[11] A.M. Maitra, N.W. Cant and D.L. Trimm, Appl. Catal. 48 (1989) 187.
[12] M.O. Alias and V. Srinivasan, Proc. Indian Acad. Sci. 102 (1990) 117.
[13] M.O. Alias and V. Srinivasan, Hung. J. Ind. Chem. 20 (1992) 161.
[14] R. Peter and M. Zdrazil, Coll. Czech. Chem. Commun. 51 (1986) 327.
[15] L. Karakonstantis, H. Matralis, Ch. Kordulis and A. Lycourghiotis, J. Catal. 162 (1996) 306.
[16] C.-H. Kim, W.L. Yoon, I.C. Lee and S.I. Woo, Appl. Catal. A 144 (1996) 159.
[17] J. Cruz Reyes, M. Avalos-Borja, R. López Cordero and A. López-Agudo, Appl. Catal. A 120 (1994) 147.
[18] A. Benítez, J. Ramírez, A. Vazquez, D. Acosta and A. López-Agudo, Appl. Catal. 133 (1995) 103.
[19] M. Suvanto, J. Räty and T.A. Pakkanen, Appl. Catal. A, in press.
[20] P. Biloen and G.T. Pott, J. Catal. 30 (1973) 169.
[21] W. Grünert, W. Mörke, R. Feldhaus and K. Anders, J. Catal. 117 (1989) 485.
[22] L. Salvati, Jr., L.E. Makovsky, J.M. Stencel, F.R. Brown and D.M. Hercules, J. Phys. Chem. 85 (1981) 3700.
[23] E. Payen, S. Kasztelan, J. Grimblot and J.P. Bonnelle, J. Mol. Struct. 143 (1986) 259.
[24] Y. Yan, Q. Xin, S. Jiang and X. Guo, J. Catal. 131 (1991) 234.
[25] B. Scheffer, P. Molhoek and J.A. Moulijn, Appl. Catal. 46 (1989) 11.

[26] R.L. Cordero, J.R. Solis, J.V.G. Ramos, A.B. Patricio and A.L. Agudo, Stud. Surf. Sci. Catal. 75 (1993) 1927.

[27] D.C. Vermaire and P.C. van Berge, J. Catal. 116 (1989) 309.

[28] B. Scheffer, P.J. Mangnus and J.A. Moulijn, J. Catal. 121 (1990) 18.

[29] E. Payen, S. Kasztelan, J. Grimblot and J.P. Bonnelle, Catal. Today 4 (1988) 57.

[30] P.J. Mangnus, A. Bos and J.A. Moulijn, J. Catal. 146 (1994) 437.

[31] R.F. Howe, Inorg. Chem. 15 (1976) 486.

[32] T.L. Brown, J. Mol. Catal. 12 (1981) 41.

[33] A. Brenner and D.A. Hucul, J. Am. Chem. Soc. 102 (1980) 2484.

[34] A. Brenner and D.A. Hucul, J. Catal. 61 (1980) 216.

[35] D.A. Hucul and A. Brenner, J. Phys. Chem. 85 (1981) 496.

[36] A. Kazusaka and R.F. Howe, J. Mol. Catal. 9 (1980) 199.

[37] A. Kazusaka and R.F. Howe, J. Catal. 63 (1980) 447.

[38] S. Sivasanker and A.V. Ramaswamy, Indian J. Technol. 21 (1983) 339.

[39] A. Zecchina, E. Escalona Platero and C. Otero Areán, Inorg. Chem. 27 (1988) 102.

[40] I.M. Baibich, F.C. Stedile, I.J.R. Baumvol, J.H.Z. dos Santos and V.E. Santarosa, Phys. Stat. Solid. (1995) 519.

[41] M. Suvanto and T.A. Pakkanen, Appl. Catal. A 166 (1998) 105.

[42] J.B. Peri and R.B. Hannan, J. Phys. Chem. 64 (1960) 1526.

[43] M.C. Kung and H.H. Kung, Catal. Rev. Sci. Eng. 27 (1985) 425.

[44] J.A. Lercher, C. Gründling and G. Eder-Mirth, Catal. Today 27 (1996) 353.

[45] C. Morterra and G. Magnacca, Catal. Today 27 (1996) 497.

[46] A. Auroux and A. Gervasini, J. Phys. Chem. 94 (1990) 6371.

[47] J. Shen, R.D. Cortright, Y. Chen and J.A. Dumesic, J. Phys. Chem. 98 (1994) 8067.

[48] R. Zhang, J. Jagiello, J.F. Hu, Z.-Q. Huang and J.A. Schwarz, Appl. Catal. A 84 (1992) 123.

[49] G. Bagnasco, J. Catal. 159 (1996) 249.

[50] M.J.F.M. Verhaak, A.J. van Dillen and J.W. Geus, Appl. Catal. A 105 (1993) 251.

[51] G.S. Sewell, E. van Steen and C.T. O'Connor, Catal. Lett. 37 (1996) 255.

[52] AutoChem 2910, Automated Catalyst Characterization System, Operator's Manual V4.xx (Micromeritics Instrument Corporation, 1998).

[53] A. Brenner and R.L. Burwell, Jr., J. Catal. 52 (1978) 353.

[54] M. Suvanto and T.A. Pakkanen, J. Mol. Catal. A 138 (1999) 211.